

# Adaptive optimization in ultrafast laser material processing

Razvan Stoian<sup>a</sup>, Alexandre Mermillod-Blondin<sup>a</sup>, Arkadi Rosenfeld<sup>a</sup>, and Ingolf V. Hertel<sup>a</sup>  
 Maria Spyridaki<sup>b</sup>, Emmanuel Koudoumas<sup>b</sup>, Costas Fotakis<sup>b</sup>,  
 Igor M. Burakov<sup>c</sup>, Nadezhda M. Bulgakova<sup>c</sup>

<sup>a</sup>Max-Born Institut für Nichtlineare Optik und Kurzzeitspektroskopie,  
 Max Born Str. 2a, D-12489 Berlin, Germany

<sup>b</sup>Institute of Electronic Structure and Laser, Foundation for Research and Technology-Hellas,  
 P.O. Box 1527, 71110 Heraklion, Greece

<sup>c</sup>Institute of Thermophysics SB RAS, 1 Acad. Lavrentyev Avenue, 630090 Novosibirsk, Russia

## ABSTRACT

Ultrafast lasers promise to become attractive and reliable tools for material processing on micro- and nanoscale. The additional possibility to temporally tailor ultrashort laser pulses by Fourier synthesis of spectral components enables extended opportunities for optimal processing of materials. An experimental demonstration of the technique showing the possibility to design particular excitation sequences tailored with respect to the individual material response will be described, laying the groundwork for adaptive optimization in materials structuring. We report recent results related to the implementation of self-learning, adaptive loops based on temporal shaping of the ultrafast laser pulses to control laser-induced phenomena for practical applications. Besides the fundamental interest, it is shown that under particular excitation conditions involving modulated excitation, the energy flow can be controlled and the material response can be guided to improve processing results. Examples are given illuminating the possibility to control and manipulate the kinetic properties of ions emitted from laser irradiated semiconductor samples using excitation sequences synchronized with the phase transformation characteristic times.

**Keywords:** femtosecond ablation, pulse shaping, adaptive optimization, material processing.

## 1. INTRODUCTION

Ultrafast lasers proved to be powerful tools for investigating physical processes on the shortest time scale, as well as for processing different materials on the scale of optical wavelengths.<sup>1-5</sup> Their potential for material processing is based on the prospect of strong localization of energy, increased controllability,<sup>1-9</sup> and reduced residual damage, fulfilling already demands for miniaturization and integration in reliable micro and nano fabrication techniques. Ultrafast lasers offer unparalleled capabilities for reduced-scale processing, taking advantage of the strong nonlinear and selective, non-thermally driven interactions, reduced heat effects, and, more recently, the unique possibility of pulse adaptive manipulation.<sup>10</sup> The technological development of rapid optical modulation devices<sup>11</sup> and the implementation of robust adaptive numerical procedures for optimization of predefined experimental outputs have allowed the generation of complex electromagnetic waveforms in the infrared and visible spectral range and have provided an efficient tool to control and manipulate the interaction between light and matter. The capability to tailor ultrafast laser pulses to desired temporal shapes exploits the large spectral bandwidth of an ultrafast laser pulse and the possibility to have complete control over the spectral characteristics of the electrical field. Temporal pulse shaping by Fourier synthesis of spectral components has been demonstrated to be an effective technique able to control and optimize a variety of physical and chemical systems using coherent light and to route specific processes in pre-specified directions. Optimal control experiments have addressed several types of physical situations, including the selective breaking of chemical bonds, the manipulation of electron transfer in biological complexes, the creation of particular molecular vibrations, the enhancement of radiative high harmonics, or the creation of ultrafast semiconductor switches.<sup>12-19</sup> Particularly for complicated physical or chemical systems, whenever the optimal optical waveform to assist a specific transition is not

straightforward, self-learning optimization procedures may deliver the most effective way to drive the systems in pre-specified states. The extreme irradiation conditions generated by ultrashort laser pulses have also allowed generating previously unexplored properties of materials around critical points. Ultrafast laser-driven phase transitions and exotic metastable states are some of the observations that point towards novel properties and the potential of obtaining singular laser machining technologies suitable for a broad range of applications. The potential spectrum ranges from quality structuring of materials for increased functionality to integration in analytical methods sensitive to particle emission or controlled ion beams for implantation purposes. These novel techniques are conceived to generate new matter properties and phases based on synergies with the material intrinsic response, unfolding new perspectives for “intelligent”, feedback-assisted processing of materials. In the specific aspect of improving and controlling the characteristics (flux, energy, angular distribution) of the ion beams induced by laser ablation for micro and optoelectronic applications (e.g. quantum dot formation at Si/SiO<sub>2</sub> interface using shallow implantation), temporal pulse shaping is particularly promising, with the potential to compensate the current deficit in the properties of the sub-keV high-flux ion beams delivered by presently available commercial techniques.

Besides enormous scientific interest, the concept of adaptive optimization can have though significant practical implications, introducing novel concepts and potential in advanced laser material processing. While the laser energy delivery rate will be adaptively adjusted to the best coupling conditions, the materials themselves will start to play an active role in the structuring process. We propose a procedure based on evolutionary algorithms using phase modulation and, subsequently, temporal pulse tailoring as a functional degree of freedom to improve the kinetic characteristics of a Si ion beam emitted from laser irradiated silicon targets at moderate fluences.<sup>20</sup> We demonstrate that by optimizing the energy delivery rate impinging on the silicon target we can take advantage of a succession of phase transformations, drive the system in specific thermodynamic states, and obtain controllable low-kinetic-energy and high-flux ion beams for practical purposes, among them ion implantation in micro- and optoelectronics. The various characteristics of the ion beams such as kinetic energy, ionization degree, and directionality will have an influence on ion implantation techniques since they can affect penetration profiles of the impurities. Essentially, in optimization experiments the measured output is fed back into an iterative learning loop until a particular excitation sequence properly adapted to the experimental conditions is determined, without initial information of the physical parameters. Since no prior knowledge of the physical aspects of the problem is required, evolutionary algorithms can be applied for finding the optimal solution for a wide class of problems, from coherent control of electronic and nuclear degrees of freedom in complex physical, chemical, and biological systems to process optimization in practical applications. Moreover, a demonstration of designing material-removal characteristics from laser-irradiated materials is appealing for a broader range of scientific and technological applications.

## 2. EXPERIMENT

Dielectric (a-SiO<sub>2</sub>) and semiconductor (Si) samples were irradiated under vacuum conditions (10<sup>-5</sup> mbar) with 180 fs pulses from an 800 nm Ti: Sapphire oscillator-amplifier laser system delivering 0.6 mJ energy per pulse at a nominal repetition rate of 1 kHz. The laser system incorporates a closed-loop programmable pulse-shaping apparatus and additional ion detection devices. The *p*-polarized laser beam was focused onto the sample surface at 24° incidence down to a spot of approximately 900 μm<sup>2</sup>. An electromechanical shutter was used to control the irradiation dose, scaling the repetition rate down to 1 Hz. The energy in the laser pulse was smoothly varied using a half-wave plate in combination with a thin film polarizer. The irradiation process was carried out under vacuum conditions (10<sup>-5</sup> mbar).

Temporal pulse tailoring<sup>11</sup> was realized by dynamically altering the spectral phase of an incident bandwidth-limited laser pulse, which is spatially dispersed and reformed in a zero-dispersion unit that includes a 640-pixel liquid crystal (LC) modulator (Jenoptik) in the Fourier plane. The use of LC-modulators in spatially dispersed beams allows phase/amplitude modulation (by controlled retardation and attenuation at each pixel position in the frequency space) introducing different optical paths to the spatially separated spectral components and, in turn, tailoring the pulses to desired temporal shapes. Our setup was used in the phase-only modulation scheme, thus keeping constant the energy in the pulse, which was then delivered in different rates. The optical modulator was inserted after the oscillator, the amplifier being seeded with the phase-modulated beam. The temporal profile of the modulated sequence was measured by second order cross-correlation with a non-modulated pulse deflected from the oscillator prior to phase modulation and seeded in the amplifier 500 ps behind.

Positively charged Si ions were detected by a linear time-of-flight<sup>21,22</sup> (TOF) mass spectrometer with the detection axis normal to the sample surface. The emitted ions were allowed to drift for 65 mm in a field-free region and then extracted into the mass spectrometer with a pulsed electric field and detected with a microsphere plate (MSP) situated at a distance of 289 mm from the target. The pulsed voltage applied on the extraction grids at different delay times with respect to the laser pulse allows the construction of the mass-resolved velocity distribution at the position of the extraction region. The TOF mass spectrometer has the additional possibility to be used without pulsed extraction, consequently suppressing the mass resolution but allowing the measurement of the flight time of the emitted charge from the target to the detector.

The variable extraction-field delay samples the expanding ablation plume temporally. The ion signal recorded for a given extraction time corresponds to a well-specified velocity of the ions.

In connection to the time-of-flight detection, the electro-mechanical shutter has the additional possibility to select groups of 5 consecutive pulses separated by 10 ms at a repetition rate of 1 Hz. The signal was recorded for the last pulse in the sequence, the initial four pulses being used to remove the native oxide layer. Each sequence illuminates a fresh spot on the surface.

### 3. RESULTS AND DISCUSSION

The possibility to synchronize the laser radiation with the material response and to realize synergies between radiation and matter has some interesting consequences for material processing. In this way materials properties will play a dynamic role in the structuring process. A temporally shaped laser pulse can induce a modulated electronic excitation with the possibility to achieve a certain degree of control for the subsequent electronically-induced structural transformations. Brittle dielectrics irradiated with temporally shaped pulses<sup>10</sup> have indicated the possibility to improve the structuring process and eliminate fracturing based on a laser-induced brittle-to-ductile transition.<sup>23</sup> The transition is regulated by the fast trapping of the electrons<sup>24-27</sup> that causes lattice deformations and transient atomic displacements, softening the irradiated surface on a sub-ps time scale. Moreover, using multipulse excitation sequences with sub-ps separation, the irradiated spot shows a spatially modulated depth profile,<sup>28</sup> consequence of modulated coupling properties as depicted in Figure 1 (a). The modulated absorption is determined dominantly by the fast, transient build-up of self-trapped excitonic states in fused silica. Theoretical modeling based on a two dimensional extension of the energy transport model developed by Bulgakova et al.<sup>29</sup> taking into account the energetic loss due to electron trapping indicates the establishment of a non-monotonous temperature profile in the sample after irradiation (Fig. 1 (b)) on ps time scale.

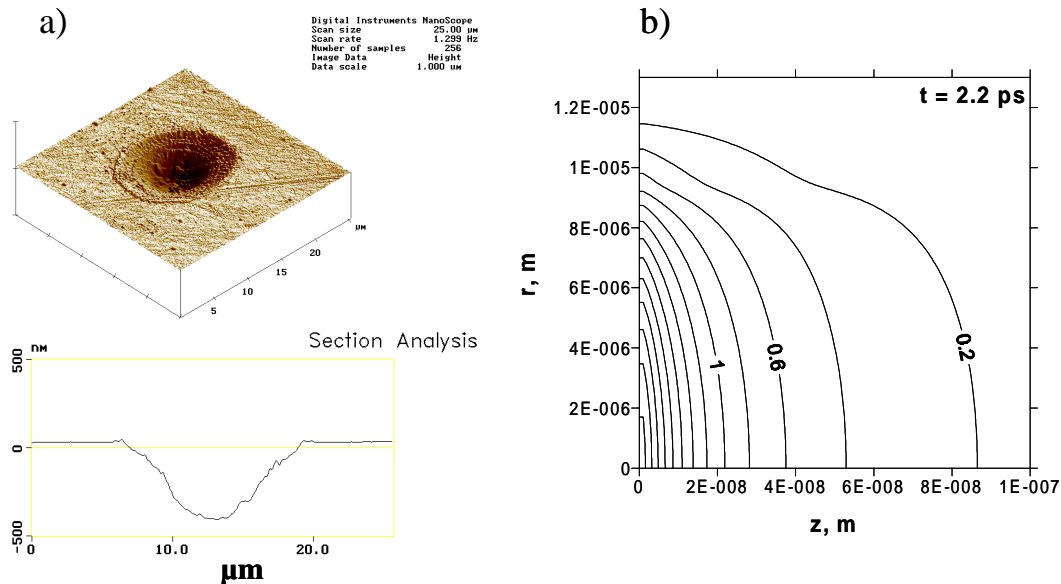


**Fig. 1.** (a) Single shot structures made on a-SiO<sub>2</sub> surfaces with triple pulses separated by 1 ps at 14 J/cm<sup>2</sup>. The temporal modulation of the pulse train leads to a modulation of the spatial profile. (b) 2D-temperature profile in the a-SiO<sub>2</sub> sample at the end of the excitation sequence.

Previous time-resolved experiments on laser-induced ion emission from different classes of materials<sup>30,31</sup> have indicated significant differences between dielectrics, semiconductors, and metals. The results have clearly demonstrated the absence of the electrostatic break-up of the surface for the last two types of materials and a significant increase of the efficiency of ion emission from silicon samples on a picosecond time scale, in very good agreement with time-resolved X-ray diffraction detection of the thermal response of the Si lattice.<sup>32,33</sup>

Semiconductor excitation by ultrafast laser irradiation<sup>34-39</sup> at fluences around the damage threshold has revealed the appearance of a high reflectivity, almost metallic-like phase upon the development of a dense electron-hole plasma with the optical response of a free electron gas. When an intense light beam, carrying photons of sufficient energy to overcome the band gap, illuminates the semiconductor, free carriers are generated via one and two-photon interband absorption followed by further free-electron heating. If a specific threshold is surpassed, the strong electronic excitation is almost immediately followed by premature bond-softening, lattice destabilization, and the appearance of non-thermal phase transitions on a sub-ps time scale. The ultrafast lattice disordering induced primarily by electronic excitation precedes the thermal phase transformations. For lower energy inputs, screened nonradiative recombination, delayed carrier-lattice thermalization, and phonon equilibration together with thermal transport limited by the sound velocity will force the characteristic time for the thermal melting on a few picoseconds timescale. Material removal proceeds via the hydrodynamic expansion of the excited matter.

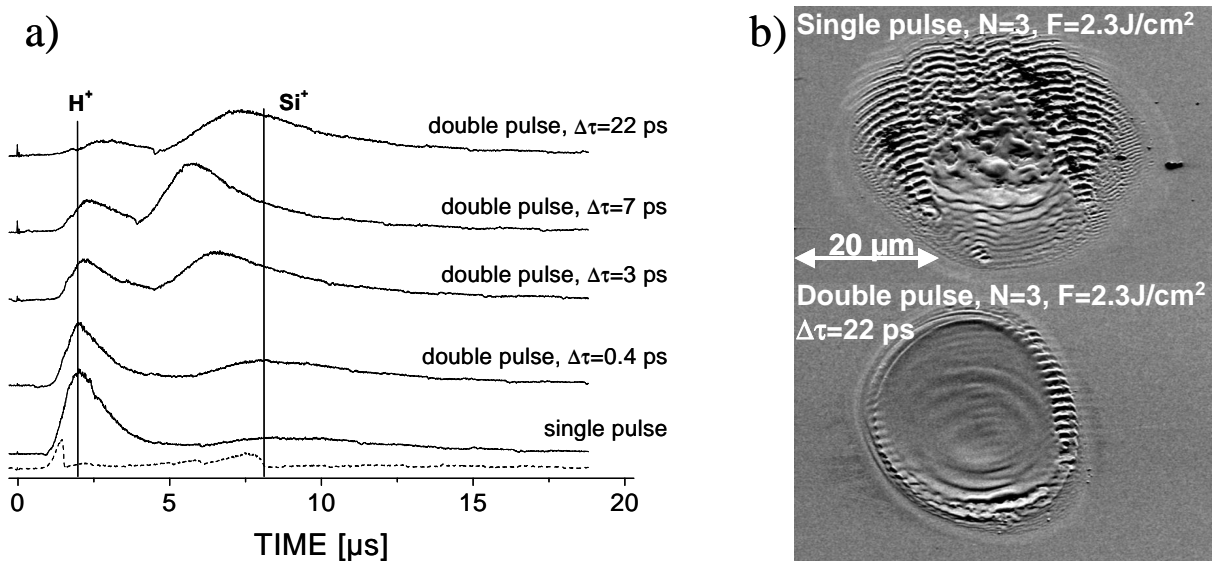


**Fig. 2.** (a) Non-mass resolved TOF ion spectra from silicon targets under ultrafast laser irradiation with single and double-pulses with increasing separation times between the two pulses, at  $0.9 \text{ J/cm}^2$  total incident fluence. To demonstrate the species content of the features, a short-range retarding positive voltage of 200 V was applied in front of the charge detector (dot lines). The results are derived from a spot previously irradiated with 6 sequences per site. (b) Scanning electron microscope images of the laser-induced structures generated after 3 successive irradiation sequences of single and double, 22 ps separated pulses of  $2.3 \text{ J/cm}^2$  total fluence on the same spot. While the single-peak irradiation generates significant melt residuals suggesting strong thermal and hydrodynamic activity, double-pulse irradiation produces cleaner structures by efficiently coupling the second pulse into the initially induced liquid region.

Directional ion emission from laser-irradiated silicon samples is an interesting candidate for pulse tailoring experiments on ps timescale due to the benefit of a succession of fast electronic and structural changes triggered by the laser radiation. For the initial experiments the samples were irradiated with double ultrafast (180 fs) pulses with equal intensities and separation distances between few hundred femtoseconds and 22 picoseconds.

Figure 2 (a) displays the TOF spectra of the detected charge without mass resolution except the rough indication given by the characteristic drift of species with different masses. The traces were recorded for single pulse interaction and 4 cases of double pulse sequences temporally separated by 0.4 ps, 3 ps, 7 ps and 22 ps but with identical energy content.

The silicon samples were repeatedly exposed to 6 excitation sequences per site at 2 Hz repetition rate and  $0.9 \text{ J/cm}^2$  total incident energy density. A double peak distribution is present with the first peak centered at around  $2 \mu\text{s}$  arrival time and containing dominantly positive hydrogen ions with energies below 300 eV. We did not observe at this moderate fluence any energetic (keV) particles as claimed in previous reports.<sup>40</sup> The hydrogen yield is a consequence of the laser-activated hydrogen emission following water dissociative adsorption on the silicon sample. The composition of the two peaks can easily be determined with the help of a positive retarding field with a short action range in front of the MSP detector having the function of a low energy filter. A 200 V retarding field removes almost entirely the first peak. The characteristic cut-off times of the barrier in the second peak indicate the presence of Si ions, mainly single ionized for single pulse irradiation. Double-pulse irradiation with picosecond separation favors, to a certain extent, the appearance of multiple ionized species and produces an evident energy gain for the single ionized silicon atoms as compared to the single pulse irradiation. The position of the second peak depends strongly on the laser energy delivery rate showing a downshift of almost  $3 \mu\text{s}$  as we increase the time separation of the two pulses, a tendency opposed to the  $\text{H}^+$  peak behavior.

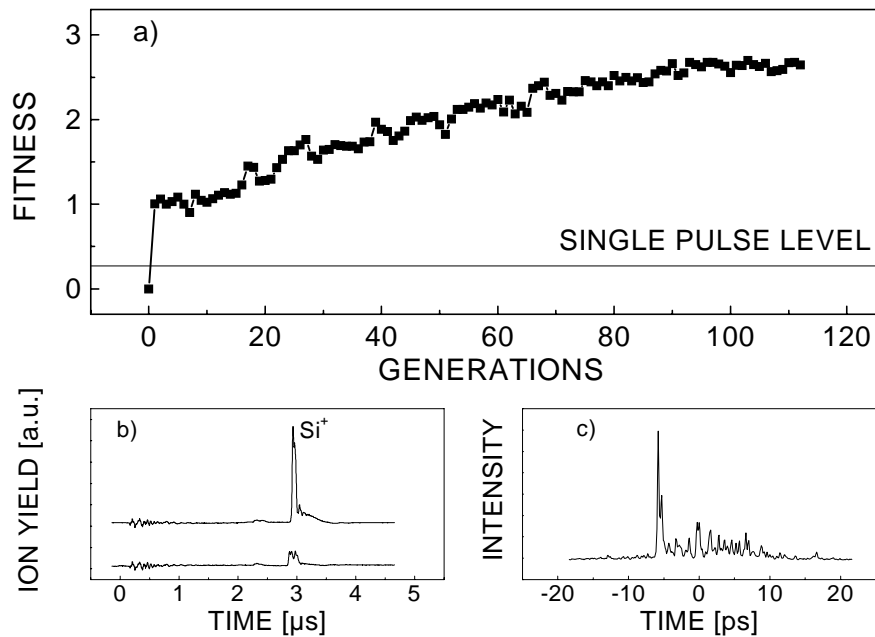


**Fig. 3.** (a) Evolution of the  $\text{Si}^+$  ion yield during the optimization run. A several fold increase is obtained for the ion yield with a velocity of  $4.5 \times 10^4 \text{ m/s}$  at a fluence of  $0.8 \text{ J/cm}^2$ . (b) The TOF mass-resolved  $\text{Si}^+$  trace corresponding to the single pulse and optimal pulse respectively. (c) The intensity envelope of the optimal pulse.

The improved efficiency of ion emission with increasing pulse separation on the picosecond scale may suggest a gas-phase interaction, though the separation times in the double-pulse sequence are too short to allow a gas-phase expansion and delayed ionization of emitted neutrals by the second pulse. Moreover, the leading pulse alone has not enough energy to induce significant material removal. Concomitantly, the morphology of the damage (Fig. 2 (b)) suggests a direct coupling to the thermally affected solid.<sup>41</sup> For separation distances longer than 3 ps the following scenario can be anticipated: The excitation induced by the first pulse degenerates into a significant melting zone with altered optical properties, characteristic to the hot, liquid silicon. The second pulse couples very efficiently to the liquid layer, leading to total vaporization of the melted front, and leaves behind a featureless structure without the residual cast (Fig. 2 (b)). In contrast, single-pulse irradiation produces significant thermal and hydrodynamic effects in the residual melt that strongly affects the quality of the structure. An optimal separation between the pulses corresponds to the formation of a liquid layer with the thickness equal to the optical penetration depth and leads to the formation of smooth structures on the surface. An additional effect concerning the efficiency of the laser energy deposition is noticed in the reduction of the

energetic gap between the observed damage threshold through local melting of the surface ( $\sim 0.2 \text{ J/cm}^2$ ) and the onset of ablation coupled with strong ion emission.

In a second round of experiments we have applied adaptive numerical schemes to optimize the kinetic properties of the ion beam.<sup>41</sup> The pulse was dynamically adapted to optimize the experimental result in a closed, self-learning loop.<sup>43</sup>

The selectivity in generating high carrier densities in semiconductor materials is reduced<sup>44</sup> since all the accessed states in the conduction band will contribute to the current flow. The selection will rely in this case on the more favorable energetic pathway with respect to the final *lattice* temperature. For irradiation doses specific to the ablation regime, rapid electronic dephasing in overcritically excited silicon severely reduces the possibility to trigger coherent processes, especially when the final state belongs to the continuum. As opposed to quantum control strategies where one tries to obtain electromagnetic fields designed to drive the system in final target quantum states, we build here on the temporal succession of different types of phase transformation adapting the laser energy delivery rate to a succession of structural changes, giving access to both ultrafast, non-thermally driven interactions, as well to classic thermal domains.

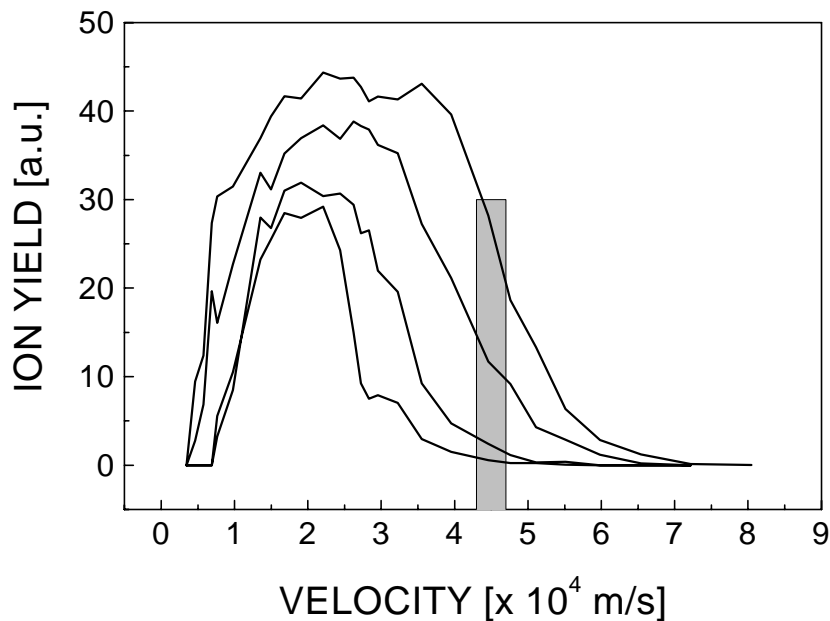


**Fig. 4.**  $\text{Si}^+$  ion velocity distributions for different target functions, showing the tunability of the kinetic properties of the ions. The fastest distribution corresponds to irradiation with the optimal pulse. The velocity window used in optimization is marked on the figure.

The amplitude of the ion signal with a chosen velocity serves as feedback for the optimization loop. To select the specific velocity, the pulsed extraction delay was set to the corresponding fixed value. The optimization of the ion yield is performed using a self-learning evolutionary strategy that produces suitable phase masks and programmable manipulation of the time-domain laser pulse envelopes. The procedure starts from a complex of arbitrary or reasonable-guess functions for the initial phase patterns applied on the optical modulator, which then evolves through genetic propagators. Evolution operators such as crossover and mutation are applied to search the solution space efficiently. Results will be ranked according to their fitness (the measured value of the quantity to be optimized, in our case the magnitude of the velocity resolved ion yield), and the algorithm will suggest an improved collection of solutions, searching the multidimensional space similar to biological evolution. For our specific purpose the optimization sequence begins with a partially random population of 50 individuals (strings corresponding to a defined phase mask on the modulator), including also the single, Fourier-transformed pulse and sometimes solutions obtained by previous runs of the algorithm. Assessing the signal, the algorithm iteratively proposes solutions based on the “survival of the fittest”

selection procedure until convergence is achieved. Details about global optimization methods describing suitable use of crossover and mutation selection rules to ensure efficient exchange of information, genetic diversity, and to prevent trapping in local minima can be found elsewhere.<sup>43</sup>

The value of the measured ion yield for an appropriate phase mask indicates the pulse capability to perform the specified task. The signal enhancement via the trial and error procedure iteratively instructs the laser to push the system in a thermodynamic state where highest temperatures can be achieved with minimal energetic losses, based on the measured success of previous pulses. Minimal information about the physical insight is required at the beginning, but the optimal pulse includes the acquired knowledge about the mechanisms of control. The limitations of the shaping device are given by the upper boundary of the shaping temporal window which relates to the spectral resolution of the zero-dispersion unit. In our case this was limited to 22 ps.

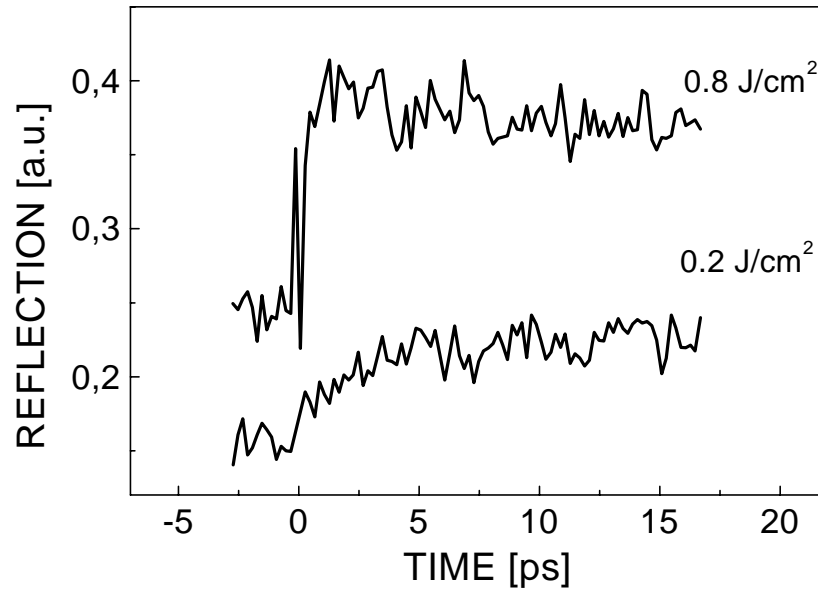


**Fig. 5.** Time-resolved reflectivity of the excited silicon surface at different irradiation doses as a probe for laser-induced electronic and structural modifications.

The result of the optimization run offers the means to understand and control the laser-induced structural modifications that transiently change the coupling properties of the incoming radiation. Improvements are achieved even when the solution space topology is very complex and the selectivity of the excitation is reduced allowing for a large class of solutions for a defined target. The algorithm is providing similar solutions as long as sufficient energy is provided. At low energies, close to the ion detection threshold, the algorithm returns a single short pulse. The results are physically meaningful since only the highest intensity provided is able to take advantage of higher order absorption to generate a sufficient electron density. The evolution of the system during the global optimization run is presented in Figure 3 (a) for a spatially averaged fluence of  $0.8 \text{ J/cm}^2$ , approximately 4 times above the observed damage threshold. The task to maximize the ion yield with the velocity of  $4.5 \times 10^4 \text{ m/s}$  (Fig. 3 (b)) with an increase of almost ten times delivers as optimal intensity envelope a sequence of two pulses; a fast, short peak followed by a long pulse after approximately 8 ps (Fig. 3 (c)). Measuring the relative energy balance between the two pulses, one finds out as an essential feature that the energy content of the first pulse (approximately 25% of the total energy) always levels out at the thermal solid-to-liquid phase transition threshold, realizing the minimal energetic requirements to induce the structural change. By judiciously redistributing the laser energy the excitation sequence prepares the irradiated region for the most effective coupling conditions. A higher energy of the initial pulse will force the non-thermal disordering, losses will be increased due to the higher reflectivity and less energy will be available to heat the residual melt. Once the liquid phase is nucleated over a depth of few nanometers, the second pulse couples always in a molten, metallic-like phase dominated by one-photon

intraband transitions. The absorption coefficient is dramatically enhanced<sup>45</sup> up to  $\alpha_{\text{liquid}}=10^8 \text{ m}^{-1}$  and the whole energy of the second pulse is deposited within the first nanometers, leading to a significant increase in the energy density confined in the liquid layer. The match between the thickness of the liquid layer and the absorption length of the pulse has also extended consequences for material structuring, a sharper temperature gradient at the liquid-solid interface being equivalent to restricting the interaction to the molten region. The ion flow is manipulated therefore by the thermally-induced transition to the molten phase and further energy deposition in the overheated liquid layer. Moreover, due to the somehow poorer electrical properties of liquid silicon as compared to a typical metal, carrier transport is inhibited and the energy has reduced means to diffuse away from the interaction region, establishing conditions to reach extremely high temperatures. To prove the case the optimal sequence was compared with the initial set of experiments using sequences of double, equal-intensity pulses separated by 10 and 22 ps with the same total energy, the recorded yield being absolutely comparable, which means that, since the one-photon absorption dominates the energy depositions in the liquid phase, the particular shape of the second pulse does not play a significant role anymore. The amount of energy deposited in the liquid layer is then simply given by  $\int_{\tau}^{\infty} R(t)I(t)dt$  where  $\tau$  denotes the onset of the phase transition and  $R(t)$  is the transient reflectivity. The velocity distribution corresponding to the optimal irradiation is presented in Fig. 4. The broad velocity envelope suggests the presence of several stream velocity components corresponding to different stages of removal. Similar fast velocity features can be induced by a single short pulse with an energy density superior to  $1.6 \text{ J/cm}^2$ . The possibility to define the fitness function according to specific targets allows one to access also the gray levels between the zero level and the maximum ion value by redistributing the energy between the two main features of the optimal pulse. Optimization of different velocity windows for the ions opens up the possibility to generate ion beams with tunable kinetic properties on the expense of the absolute number of ions produced. Figure 4 shows several velocity distributions covering a large spectrum of accessible energies for the emitted ions when temporally-selective excitation is used, allowing for the accurate control of the degree of superheating.

To confirm the real-time development of the laser-triggered processes we have performed a time-resolved experiment detecting the reflected part of a *p*-polarized weak probe pulse in a cross-polarized, collinear pump-probe setup after previous excitation with short singular pulses with different amounts of energy. The irradiation geometry was kept similar to the optimization experiment. The 25° laser incidence enables good discrimination between the electronic and structural changes. To preserve the experimental conditions, no particular care has been taken to match the size of the probe with the region of uniform excitation, the recorded signal corresponding to the spatially-averaged reflectivity. Though the reflectivities alone cannot provide the complete picture, corroborated with previously reported imaging experiments<sup>35,37</sup> and time-resolved X-ray detection<sup>32,33</sup>, one can obtain a satisfactory prognosis. At low input energies, close to the melting threshold and equal to the energy content of the first peak in the optimal sequence, a slow increase of the reflectivity is observed, which levels out after more than 5 ps. Increasing the pump energy, the situation gradually changes, culminating with the appearance of the fast, sub-ps non-thermal transition to the disordered phase (Fig. 5). Replacing the initially short pump pulse with the optimal excitation sequence indicated a slow increase of the reflectivity, peaking up 8 ps after the initial spike confirming the temporal development of the energy coupling. For this last set of measurements, a second oscillator pulse bypassing the modulator was injected into the amplifier 0.5 ns delayed with respect to the modulated pulse and used as a probe.

#### 4. CONCLUSIONS

In conclusion we have presented experimental results related to the influence of temporal shaping of ultrafast laser pulses on laser-irradiated materials above the ablation threshold. Besides a brief review of applications for processing of dielectric materials, examples were given to illustrate the possibility to manipulate the properties of ion beams generated during laser ablation of Si wafers. In a first set of experiments we have shown a significant increase in the emitted ion yield from silicon surfaces when double-pulse sequences with separations on the time scale of the solid-to-liquid thermal phase transformation are used.

In a second set of experiments we have also demonstrated that adaptive evolutionary optimization schemes and pulse temporal tailoring can have an extended range of action, enabling applications that could largely benefit from the synergies between the laser action and the material characteristic response. Our results show that is possible to adaptively optimize the kinetic properties of ions emitted from laser irradiated semiconductor samples using excitation sequences synchronized with the phase transformation characteristic times. It was shown that under particular excitation conditions involving modulated excitation, the energy flow can be controlled and the material response can be guided to



improve processing results. This study demonstrates the additional advantages of utilizing temporally tailored ultrafast laser pulses, laying the basis for the possibility of generating ion beams with specific energetic properties whenever optimally designed excitation pulses are used for irradiation.

## 5. ACKNOWLEDGEMENTS

The EU Access to research infrastructure programs under the contracts HPRI-CT-1999-00084 and HPRI-CT-2001-00139 and the Wissenschaftlich-Technologischen Zusammenarbeit (WTZ) project RUS01/224 are gratefully acknowledged.

## REFERENCES

1. E. N. Glezer and E. Mazur, "Ultrafast-laser driven micro-explosions in transparent materials", *Appl. Phys. Lett.* **71**, pp. 882-884, 1997.
2. F. Korte, S. Nolte, B. N. Chichkov, T. Bauer, G. Kamlage, T. Wagner, C. Fallnich, and H. Welling, "Far-field and near-field material processing with femtosecond laser pulses", *Appl. Phys. A: Mater. Sci. Process.* **69**, pp. S7-S11, 1999.
3. X. Liu, D. Du, and G. Mourou, "Laser ablation and micromachining with ultrashort laser pulses", *IEEE J. Quantum. Elec.* **33**, pp. 1706-1716, 1997.
4. M. Lezner, J. Krüger, S. Sartania, Z. Cheng, Ch. Spielmann, G. Mourou, W. Kautek, and F. Krausz, "Femtosecond optical breakdown in dielectrics", *Phys. Rev. Lett.* **80**, pp. 4076-4079, 1998.
5. F. Korte, S. Adams, A. Egbert, C. Fallnich, and A. Ostendorf, "Sub-diffraction limited structuring of solid targets with femtosecond laser pulses" *Opt. Exp.* **7**, pp. 41-49, 2000.
6. B. C. Stuart, M. D. Feit, A. M. Rubenchik, B. W. Shore, and M. D. Perry, "Laser-induced damage in dielectrics with nanosecond to subpicosecond pulses", *Phys. Rev. Lett.* **74**, pp. 2248-2251, 1995.
7. A.-C. Tien, S. Backus, H. C. Kapteyn, M. M. Murnane, and G. Mourou, "Short-pulse laser damage in transparent materials as a function of pulse duration", *Phys. Rev. Lett.* **82**, pp. 3883-3886, 1999.
8. D. Ashkenasi, H. Varel, A. Rosenfeld, F. Noack, and E.E.B. Campbell, "Pulse-width influence on laser structuring of dielectrics", *Nucl. Instr. Meth. B* **122**, pp. 359-363, 1997.
9. H. Varel, D. Ashkenasi, A. Rosenfeld, Herrmann R, F. Noack, and E. E. B. Campbell, "Laser-induced damage in SiO<sub>2</sub> and CaF<sub>2</sub> with picosecond and femtosecond laser pulses", *Appl. Phys. A: Mater. Sci. Process.* **62**, pp. 293-294, 1996.
10. R. Stoian, M. Boyle, A. Thoss, A. Rosenfeld, G. Korn, E. E. B. Campbell and I. V. Hertel, "Laser ablation of dielectrics with temporally shaped femtosecond pulses", *Appl. Phys. Lett.* **80**, pp. 353-355, 2002.
11. A. M. Weiner, "Femtosecond Pulse Shaping Using Spatial Light Modulators", *Rev. Sci Instrum.* **71**, pp. 1929-1960, 2000.
12. J. P. Heritage, R. N. Thurston, W. J. Tomlinson, A. M. Weiner, and R. H. Stollen, "Spectral windowing of frequency-modulated optical pulses in a grating compressor", *Appl. Phys. Lett.* **47**, pp. 87-89, 1985.
13. R. S. Judson and H. Rabitz, "Teaching lasers to control molecules" *Phys. Rev. Lett.* **68**, pp. 1500-1503, 1992.
14. D. Meshulach and Y. Silberberg, "Coherent quantum control of two-photon transitions by a femtosecond laser pulse", *Nature* **396**, pp. 239-242, 1998.
15. T. C. Weinacht, R. Bartels, S. Backus, P. H. Bucksbaum, B. Pearson, J. M. Geremia, H. Rabitz, H. C. Kapteyn, and M. M. Murnane, "Coherent learning control of vibrational motion in room temperature molecular gases", *Chem. Phys. Lett.* **344**, pp. 333-338, 2001.

16. T. Feurer, J. C. Vaughan, and K. A. Nelson, "Spatiotemporal coherent control of lattice vibrational waves", *Science* **299**, pp. 374-377, 2003.
17. A. Assion, T. Baumert, M. Bergt, T. Brixner, B. Kiefer, V. Seyfried, M. Strehle, and G. Gerber, "Control of chemical reactions by feedback-optimized phase-shaped femtosecond laser pulses", *Science* **282**, pp. 919-922, 1998.
18. R. Bartels, S. Backus, E. Zeek, L. Misoguti, G. Vdovin, I.P. Christov, M.M. Murnane, and H.C. Kapteyn, "Shaped-pulse optimization of coherent emission of high-harmonic soft X-rays," *Nature* **406**, pp. 164-166, 2000.
19. J. Kunde, B. Baumann, S. Arlt, F. Morier-Genoud, U. Siegner, and U. Keller, "Optimization of adaptive feedback control for ultrafast semiconductor spectroscopy" *J. Opt. Soc. Am. B* **18**, 872, 2001.
20. M. Spyridaki, E. Koudoumas, P. Tzanetakis, C. Fotakis, R. Stoian, A. Rosenfeld, and I. V. Hertel, "Temporal pulse manipulation and ion generation in ultrafast laser ablation of silicon", *Appl. Phys. Lett.* **83**, 1474-1476, 2003.
21. H. Varel, M. Wahmer, A. Rosenfeld, D. Ashkenasi, and E. E. B. Campbell, "Femtosecond laser ablation of sapphire: time-of-flight analysis of ablation plume", *Appl. Surf. Sci.* **127-129** pp. 128-133, 1998.
22. R. Stoian, H. Varel, A. Rosenfeld, D. Ashkenasi, R. Kelly, and E.E.B. Campbell, "Ion time-of-flight analysis of ultrashort pulsed laser-induced processing of Al<sub>2</sub>O<sub>3</sub>", *Appl. Surf. Sci.* **165**, pp. 44-55, 2000.
23. J. Siegel, K. Ettrich, E. Welsch, and E. Matthias, "UV-laser ablation of ductile and brittle metal films", *Appl. Phys. A* **64**, pp. 213-218, 1997.
24. S. Guizard, P. D'Oliveira, P. Daguzan, P. Martin, P. Meynadier, and G. Petite, "Time-resolved studies of carriers dynamics in wide band gap materials", *Nucl. Instr. Meth. Phys. B* **116**, pp. 43-48, 1996.
25. F. Quere, S. Guizard, P. Martin, G. Petite, O. Gobert, P. Meynadier, and M. Perdrix, "Ultrafast carrier dynamics in laser-excited materials: subpicosecond optical studies", *Appl. Phys. B Lasers O*, **68**, pp. 459-463, 1999.
26. M. Li, S. Menon, J. P. Nibarger, and G. N. Gibson, "Ultrafast electron dynamics in femtosecond optical breakdown of dielectrics", *Phys. Rev. Lett.* **82**, pp. 2394-2397, 1999.
27. R. Lindner, M. Reichling, R. T. Williams, E. Matthias, "Femtosecond laser pulse excitation of electrons and excitons in CaF<sub>2</sub> and SrF<sub>2</sub>", *J. Phys.: Condens. Matter* **13**, pp. 2339-2346, 2001.
28. R. Stoian, M. Boyle, A. Thoss, A. Rosenfeld, G. Korn, and I.V. Hertel, "Dynamic temporal pulse shaping in advanced ultrafast laser material processing", *Appl. Phys. A* **77**, pp. 265-269, 2003.
29. N. M. Bulgakova, R. Stoian, A. Rosenfeld, I. V. Hertel, and E. E. B. Campbell "Electronic transport and consequences for material removal in ultrafast pulsed laser ablation of materials", *Phys. Rev. B* **69**, 054102 (2004).
30. R. Stoian, A. Rosenfeld, D. Ashkenasi, I. V. Hertel, N. M. Bulgakova, and E. E. B. Campbell, "Surface charging and impulsive ion ejection during ultrashort pulsed laser ablation", *Phys. Rev. Lett.* **88**, 097603, 2002.
31. R. Stoian, D. Ashkenasi, A. Rosenfeld, and E. E. B. Campbell, "Coulomb explosion in ultrashort pulsed laser ablation of Al<sub>2</sub>O<sub>3</sub>", *Phys. Rev. B.* **62**, pp. 13167-13173, 2000.
32. C. W. Siders, A. Cavalleri, K. Sokolowski-Tinten, C. Toth, T. Guo, M. Kammler, M. H. von Hoegen, K. R. Wilson, D. von der Linde, and C. P. J. Barty, "Detection of nonthermal melting by ultrafast X-ray diffraction", *Science* **286**, pp. 1340-1342, 1999.
33. A. Rousse, C. Rischel, S. Fourmaux, I. Uschmann, S. Sebban, G. Grillon, P. Balcou, E. Foster, J. P. Geindre, P. Audebert, J. C. Gauthier, and D. Hulin "Non-thermal melting in semiconductors measured at femtosecond resolution", *Nature* **410**, pp. 65-68, 2001.
34. J. P. Callan, A. M. -T. Kim, C. A. D. Roeser, and E. Mazur, "Universal dynamics during and after ultrafast laser-induced semiconductor-to-metal transitions", *Phys. Rev. B* **64**, 073201, 2001.
35. C. V. Shank, R. Yen, and C. Hirlimann, "Femtosecond-Time-Resolved Surface Structural Dynamics of Optically Excited Silicon", *Phys. Rev. Lett.* **51**, pp. 900-902, 1983.
36. P. Stampfli and K. H. Bennemann, "Theory for the time dependence of the laser-induced instability of the diamond structure of Si and GaAs", *J. Phys.: Condens. Matter* **5**, pp. A173-A174, 1993.

37. K. Sokolowski-Tinten, J. Bialkowski, A. Cavalleri, D. von der Linde, A. Oparin, J. Meyer-ter-Vehn, S. I. Anisimov, "Transient States of Matter during Short Pulse Laser Ablation", *Phys. Rev. Lett.* **81**, pp. 224-227, 1998.
38. K. Sokolowski-Tinten, J. Solis, J. Bialkowski, J. Siegel, C. N. Afonso, D. von der Linde D, "Dynamics of ultrafast phase changes in amorphous GeSb films", *Phys. Rev. Lett.* **81**, pp. 3679-3682, 1998.
39. K. Sokolowsky-Tinten and D. von der Linde, "Generation of dense electron-hole plasmas in silicon " *Phys. Rev. B* **61**, pp. 2643-2650, 2000.
40. S. Amoruso, X. Wang, C. Altucci, C. de Lisio, M. Armenante, R. Bruzzese, and R. Veletta, "Thermal and nonthermal ion emission during high-fluence femtosecond laser ablation of metallic targets", *Appl. Phys. Lett.* **77**, pp. 3728-3730, 2000.
41. T. Y. Choi, D.J. Hwang, C. P. Grigoropoulos, „Femtosecond laser induced ablation of crystalline silicon upon double beam irradiation“, *Appl. Surf. Sci.* **197-198**, pp. 720-725, 2002.
42. R. Stoian, A. Mermillod-Blondin, A. Rosenfeld, I. V. Hertel, M. Spyridaki, E. Koudoumas, P. Tzanetakis, C. Fotakis, and N. M. Bulgakova, in preparation.
43. A. Bartelt, Ph.D. Thesis Freie Universität Berlin (2002).
44. A. Hache, Y. Kostoulas, R. Atanasov, J. L. P. Hughes, J. E. Sipe, and H. M. van Driel, "Observation of Coherently Controlled Photocurrent in Unbiased, Bulk GaAs", *Phys. Rev. Lett.* **78**, pp. 306-309, 1997.
45. G. E. Jellison and D. H. Lowndes, "Measurements of the optical properties of liquid silicon and germanium using nanosecond time-resolved ellipsometry", *Appl. Phys. Lett.* **51**, pp. 352-354, 1987.